Rapid Communications

Correlation between compensation temperatures of magnetization and angular momentum in GdFeCo ferrimagnets

Yuushou Hirata,[1] Duck-Ho Kim,[1,*] Takaya Okuno,[1] Tomoe Nishimura,[1] Dae-Yun Kim,[2] Yasuhiro Futakawa,[3] Hiroki Yoshikawa,[3] Arata Tsukamoto,[3] Kab-Jin Kim,[4] Sug-Bong Choe,[2] and Teruo Ono[1,5,†]

[1]*Institute for Chemical Research, Kyoto University, Uji, Kyoto 611-0011, Japan*

[2]*Department of Physics and Institute of Applied Physics, Seoul National University, Seoul 08826, Republic of Korea*

[3]*College of Science and Technology, Nihon University, Funabashi, Chiba 274-8501, Japan*

[4]*Department of Physics, Korea Advanced Institute of Science and Technology, Daejeon 34141, Republic of Korea*

[5]*Center for Spintronics Research Network, Graduate School of Engineering Science, Osaka University, Machikaneyama 1-3, Toyonaka, Osaka 560-8531, Japan*

(Received 18 October 2017; published 12 June 2018; corrected 10 August 2018 and 27 February 2019)

Determining the angular momentum compensation temperature of ferrimagnets is an important step towards ferrimagnetic spintronics, but it is not generally easy to achieve it experimentally. We propose a way to estimate the angular momentum compensation temperature of ferrimagnets without a dynamical characterization technique. We derive a simple equation that relates the magnetization compensation temperature, the Curie temperature, and the angular momentum compensation temperature based on the critical exponent approximation. We show that the derived equation can explain our experimental results and can be used to estimate the angular momentum compensation temperature from the temperature dependence of magnetization.

DOI: 10.1103/PhysRevB.97.220403

I. INTRODUCTION

Antiferromagnets came into the spotlight in the last decade [1–6] as a promising material for spintronics devices because they exhibit fast magnetic dynamics and low susceptibility to magnetic fields. These advantages originate from the antiferromagnetic ordering in which the magnetic moments are compensated on an atomic scale. This also implies that it is difficult to efficiently manipulate antiferromagnets using external magnetic fields, hindering the study of antiferromagnetic spin dynamics. However, recently, magnetic-field-controlled antiferromagnetic spin dynamics has been achieved using ferrimagnets [7]. Hence, ferrimagnets have become a promising material in the emerging field of antiferromagnetic spintronics.

Ferrimagnetic materials comprise rare-earth (RE) and transition-metal (TM) compounds, wherein the spins of two inequivalent sublattices are coupled antiferromagnetically [8–10]. Because of the different Landé g factors of the RE and TM elements, ferrimagnets exhibit compensation temperatures of magnetization and angular momentum [11], at which the magnetizations (angular momenta) of the RE and TM sublattices have the same magnitude but opposite directions. Consequently, the net magnetization (angular momentum) is compensated. The compensation temperatures have been studied experimentally and theoretically [7,12–23]. In particular, Kim *et al.* recently observed fast field-driven domain wall (DW) motion in the vicinity of the compensation temperature of the angular momentum [7]. This observation reveals that ferrimagnets exhibit antiferromagnetic dynamics because of the zero net angular momentum at the compensation temperature of the angular momentum, even though they have magnetic moments. Although remarkable efforts have been made theoretically and experimentally [7,12–23] in understanding the role of angular momentum compensation in DW dynamics, it is difficult to determine the angular momentum compensation temperature because of the methodological complexities, impeding the rapid development of this exciting research field as well as the fundamental understanding of the compensation temperatures.

In this Rapid Communication, we report the correlation between the angular momentum and magnetization compensation temperatures in ferrimagnetic GdFeCo alloys. It is experimentally demonstrated that the angular momentum compensation temperature is directly related to the magnetization compensation temperature, regardless of the sample structures. The results show that there exists a strong correlation between the two types of compensation temperatures. We theoretically verified the correlation on the basis of a simple modeling technique. Moreover, the proposed approach is a different method of determining the angular momentum compensation temperature.

II. SAMPLE FABRICATION AND EXPERIMENTAL SETUP

For this study, we prepared six types of amorphous ferrimagnet GdFeCo films. Table I lists the detailed sample structures. The films were grown by cosputtering, and the compositions were estimated from the relative deposition rates of Gd and FeCo. The samples exhibit perpendicular magnetic anisotropy (PMA) with circular domain expansion. As shown in Fig. 1(a), an e-beam lithography technique was applied to the structural devices with a Hall bar geometry in order to detect the anomalous Hall resistance.

*Corresponding author: uzes.physics@gmail.com
†Corresponding author: ono@scl.kyoto-u.ac.jp

TABLE I. Summary of the sample structures.

	Sample structures
Sample I	5-nm SiN/20-nm $Gd_{23.5}Fe_{66.9}Co_{9.6}$/100-nm SiN/Si substrate
Sample II	5-nm SiN/30-nm $Gd_{23.5}Fe_{66.9}Co_{9.6}$/100-nm SiN/Si substrate
Sample III	5-nm SiN/1-nm Gd/5-nm $Gd_{23}Fe_{67.3}Co_{9.7}$/1-nm Gd/100-nm SiN/Si substrate
Sample IV	5-nm SiN/30-nm $Gd_{23}Fe_{67.4}Co_{9.6}$/5-nm Cu/5-nm SiN/Si substrate
Sample V	5-nm SiN/30-nm $Gd_{23}Fe_{67.4}Co_{9.6}$/5-nm SiN/Si substrate
Sample VI	5-nm SiN/20-nm $Gd_{23.5}Fe_{66.9}Co_{9.6}$/5-nm Pt/100-nm SiN/Si substrate

First, we characterized the magnetic properties of the GdFeCo samples. Figure 1(b) shows the hysteresis loop of the GdFeCo microstrip. The anomalous Hall resistance R_H is measured as a function of the perpendicular magnetic field H_z at room temperature. The clear, square hysteresis loop shows that the GdFeCo samples have strong PMA. The orange-colored arrow represents the magnetization switching field, which is referred to as the coercive field H_c.

To determine the magnetization compensation temperature T_M, we measured R_H by sweeping H_z at each temperature [7,18,20,23]. The magnetotransport properties are dominated by the FeCo moment because the energy of the $4f$ shell of Gd is located far below the Fermi energy level [23]. A sign change in R_H indicates a change in the direction of the FeCo moment. Using R_H as a function of H_z, we define the Hall resistance difference as $\Delta R_H \equiv R_H(+H_{z,sat}) - R_H(-H_{z,sat})$ [see Fig. 1(b)]. Figure 2(a) shows the Hall resistance difference ΔR_H as a function of the temperature T for sample II, where $+H_{z,sat}$ and $-H_{z,sat}$ are the saturation fields with the condition $H_c < H_{z,sat}$ [see the inset of Fig. 1(b)]. ΔR_H to zero determines $T_M = 160$ K, indicated by a blue dot.

To determine T_A, we measured the field-driven DW speed as a function of the temperature, as proposed elsewhere [7]. We first applied a sufficiently strong magnetic field with a magnitude of -200 mT ($-H_{z,sat}$) to saturate the magnetization along the $-z$ direction, and, subsequently, a constant H_z for driving the DW. H_z is selected to be lower than H_c, to eliminate the nucleation of the domain. Next, we applied a dc current I_x along the wire to detect the Hall signal [see the red arrow in Fig. 1(a)], where I_x is sufficiently small to prevent spin torques and the Joule heating effect [24–26]. We then injected a current

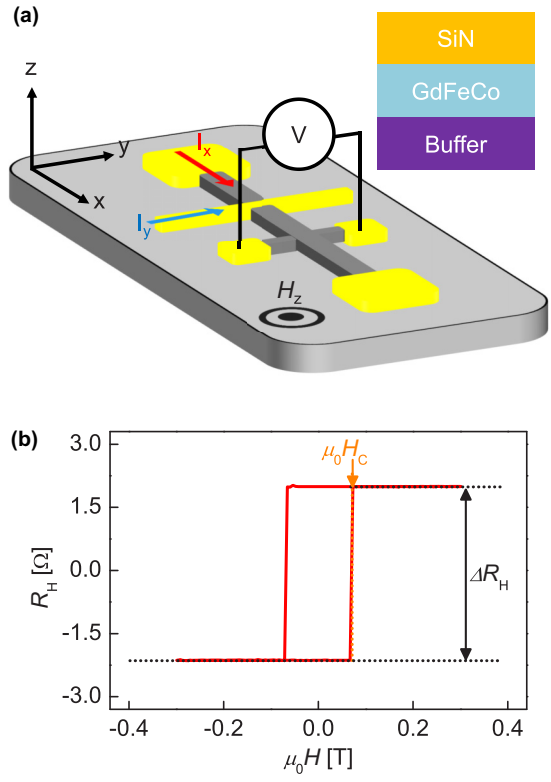

FIG. 1. (a) Schematic of the GdFeCo microwire device, and (b) anomalous Hall effect resistance R_H as a function of the perpendicular magnetic field $\mu_0 H_z$ at room temperature (300 K). The orange arrow indicates the coercive field $\mu_0 H_c$ and the black up-down arrow indicates the Hall resistance difference $\Delta R_H \equiv R_H(+\mu_0 H_{z,sat}) - R_H(-\mu_0 H_{z,sat})$, where $+\mu_0 H_{z,sat}$ and $-\mu_0 H_{z,sat}$ are the saturation fields with the condition $\mu_0 H_c < \mu_0 H_{z,sat}$.

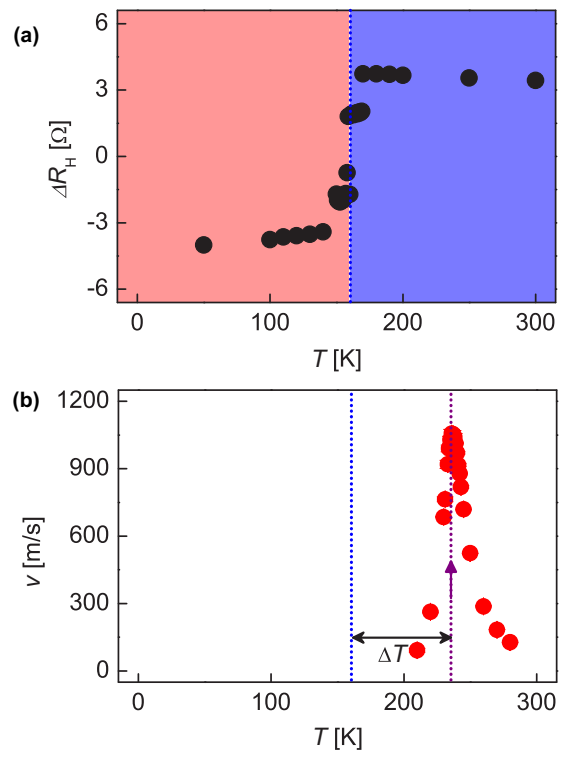

FIG. 2. (a) ΔR_H as a function of the temperature T for sample II. The blue dot indicates the magnetization compensation temperature T_M, and (b) DW speed v as a function of T for sample II at $\mu_0 H_z = 80$ mT. The blue dot indicates the magnetization compensation temperature T_M, and the purple arrow indicates the angular momentum compensation temperature T_A.

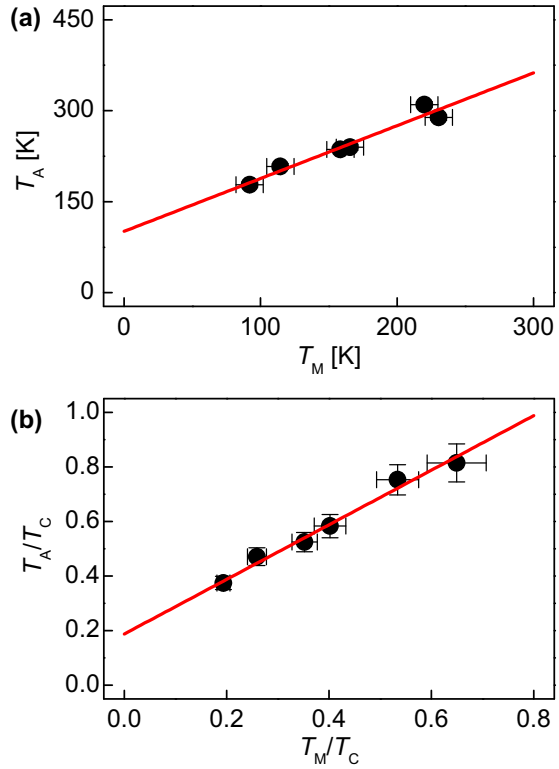

FIG. 3. (a) T_A with respect to T_M. The red line is the best linear fit. (b) T_A/T_C with respect to T_M/T_C. The red line is the best linear fit.

pulse I_y (12 V, 100 ns) through the writing line [see the blue arrow in Fig. 1(a)] to nucleate the reversed domain, thereby creating two DWs in the wire. The created DW moves along the wire because of the presence of H_z, and then passes through the Hall bar; the DW arrival time can be detected by monitoring the change in the Hall voltage using an oscilloscope. The DW speed can be calculated from the arrival time and the distance traveled between the writing line and the Hall bar (400 μm).

III. RESULTS AND DISCUSSION

Figure 2(b) shows the DW speed v as a function of the temperature T at $\mu_0 H_z = 80$ mT for sample II. This figure clearly shows that v exhibits a peak at a certain temperature (indicated by the purple arrow). This tendency of v with respect to T is consistent with the results given elsewhere [7]. Accordingly, T_A can be determined as shown in Fig. 2(b). Here, the difference between T_A and T_M is defined as ΔT ($\equiv T_A - T_M$), indicated by the black double arrows.

For a quantitative comparison, the values of T_A are directly plotted with respect to T_M for all the samples, as shown in Fig. 3(a). It is interesting to note that all the values (T_M, T_A) lie on a single curve with linearity. The red line represents the best linear fit with a slope of 0.87 and a y-axis intercept of 101.1 K. From this result, we experimentally found that there exists a strong correlation between T_M and T_A for all the GdFeCo films.

To understand the correlation of (T_M, T_A), we employ a theory based on a power-law criticality, given that the variation in the magnetization as a function of the temperature can be reasonably well approximated [27–29]. This function describes the temperature dependence of the magnetization, which can be expressed as $M(T) \sim (T_C - T)^{\beta}$, where M is the saturation magnetization, T_C is the Curie temperature, and β is the critical exponent. Accordingly, the temperature dependencies of the magnetization for Gd and FeCo can be written as $M_{Gd}(T) = M_{Gd}(0)(1 - T/T_C)^{\beta_{Gd}}$ and $M_{FeCo}(T) = M_{FeCo}(0)(1 - T/T_C)^{\beta_{FeCo}}$, respectively, where β_{Gd} (or β_{FeCo}) is the critical exponents of Gd (or FeCo) and $M_{Gd}(0)$ [or $M_{FeCo}(0)$] is the saturation magnetization of Gd (or FeCo) at zero temperature, where $\beta_{Gd} > \beta_{FeCo}$ and $M_{Gd}(0) > M_{FeCo}(0)$ [27,28]. The total saturation magnetization M_{total} can be determined using the relation $M_{total}(T) = M_{FeCo}(0)(1 - T/T_C)^{\beta_{FeCo}} - M_{Gd}(0)(1 - T/T_C)^{\beta_{Gd}}$. As $M_{total} = 0$ at $T = T_M$, the following equation can be written,

$$T_C - T_M = T_C[M_{Gd}(0)/M_{FeCo}(0)]^{1/(\beta_{FeCo} - \beta_{Gd})}. \quad (1)$$

Similarly, the total angular momentum $A_{total}(T)$ can be given as $A_{total}(T) = [M_{FeCo}(0)/\gamma_{FeCo}](1 - T/T_C)^{\beta_{FeCo}} - [M_{Gd}(0)/\gamma_{Gd}](1 - T/T_C)^{\beta_{Gd}}$, where γ_{Gd} (or γ_{FeCo}) is the gyromagnetic ratio of Gd (or FeCo). The gyromagnetic ratio of Gd (or FeCo) can be defined as $\gamma_{Gd} = g_{Gd}\frac{\mu_B}{\hbar}$ (or $\gamma_{FeCo} = g_{FeCo}\frac{\mu_B}{\hbar}$), where g_{Gd} (or g_{FeCo}) is the Landé g factor of Gd (or FeCo), μ_B is the Bohr magneton, and $\hbar$ is the reduced Plank's constant. As $A_{total} = 0$ at $T = T_A$, the following equation is obtained,

$$T_C - T_A = T_C\{[M_{Gd}(0)g_{FeCo}]/[M_{FeCo}(0)g_{Gd}]\}^{\frac{1}{(\beta_{FeCo} - \beta_{Gd})}}. \quad (2)$$

By subtracting Eq. (1) from Eq. (2), we can write the relationship between T_A and T_M as follows,

$$T_A = T_M + T_C\left[1 - (g_{FeCo}/g_{Gd})^{\frac{1}{(\beta_{FeCo} - \beta_{Gd})}}\right] \times [M_{Gd}(0)/M_{FeCo}(0)]^{\frac{1}{(\beta_{FeCo} - \beta_{Gd})}}. \quad (3)$$

Because of the spin-orbit coupling of FeCo and zero orbital angular momentum of Gd, it is known that g_{FeCo} (~ 2.2) is slightly greater than g_{Gd} (~ 2) [30–32]. Consequently, we can expect that $T_A > T_M$ due to the condition of $\beta_{Gd} > \beta_{FeCo}$, $M_{Gd}(0) > M_{FeCo}(0)$, and $g_{FeCo} > g_{Gd}$ [27,28,30–32]. From Eq. (3), the linearity of (T_M, T_A) can be easily understood. It is noteworthy that T_A depends on T_C in Eq. (3), and therefore T_C affects ΔT. This results in a slight deviation from linearity. A standard scaling treatment is employed to examine the universal behaviors. By scaling Eq. (3) and dividing it by T_C, we can obtain the relation $T_A/T_C = T_M/T_C + \eta$, where

$$\eta \equiv \left[1 - (g_{FeCo}/g_{Gd})^{\frac{1}{(\beta_{FeCo} - \beta_{Gd})}}\right][M_{Gd}(0)/M_{FeCo}(0)]^{\frac{1}{(\beta_{FeCo} - \beta_{Gd})}}. \quad (4)$$

Equation (4) shows that T_A/T_C is directly proportional to T_M/T_C when η is constant.

To confirm the above theoretical prediction, we measured T_C for each sample, as listed in Table II by performing the temperature dependence of the R_H [33]. Figure 3(b) shows the variation in T_A/T_C with respect to T_M/T_C. This relationship is clearly linear. The slope and y-axis intercept of the best linear fit are 0.99 ± 0.06 and 0.19 ± 0.02, respectively, implying that η is approximately constant for the samples with different T_C and T_A.

η for each sample can be calculated from the material parameters g_{FeCo}, g_{Gd}, $M_{Gd}(0)$, $M_{FeCo}(0)$, β_{Gd}, and β_{FeCo}. g_{FeCo}

TABLE II. Curie temperature T_C for each sample (units: K).

	Sample I	Sample II	Sample III	Sample IV	Sample V	Sample VI
T_C	475 ± 10	450 ± 10	355 ± 10	412 ± 10	412 ± 10	441 ± 10

and g_{Gd} can be referred to the literature [30–32], and the other parameters can be estimated from the temperature dependence of magnetization [7,27,28,34]. Here, we explain how to estimate η from the temperature dependence of magnetization. Figure 4(a) shows the total magnetization of GdFeCo film (sample II) as a function of temperature T, indicating that the magnetization compensation temperature T_M locates at $T = 189$ K. Since the temperature dependence of the magnetization can be expressed as a simple power-law criticality, the magnetization of RE-TM elements can be expressed as $M_{RE}(T) = M_{RE}(0)(1 - T/T_C)^{\beta_{RE}}$ and $M_{TM}(T) = M_{TM}(0)(1 - T/T_C)^{\beta_{TM}}$, respectively. Here, β_{RE} (or β_{TM}) is the critical exponents of the RE element (or TM element) and $M_{RE}(0)$ [or $M_{TM}(0)$] is the saturation magnetization of the RE element (or TM element) at zero temperature. Then, the total magnetization $M_{net}(T) = M_{TM}(T) - M_{RE}(T)$ can be expressed as

$$M_{net}(T) = M_{TM}(0)(1 - T/T_C)^{\beta_{TM}} - M_{RE}(0)(1 - T/T_C)^{\beta_{RE}}. \tag{5}$$

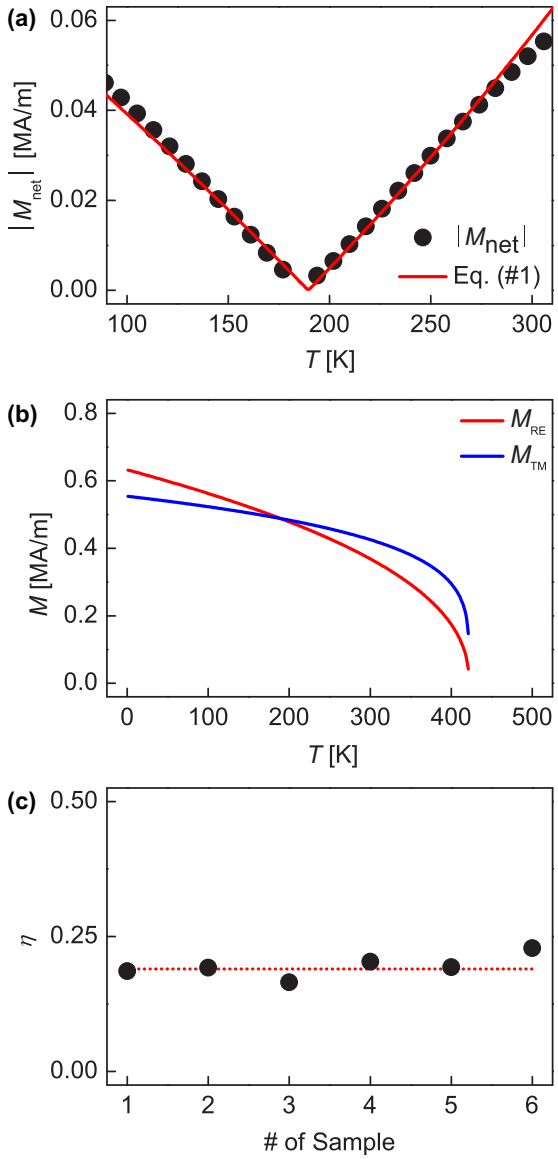

FIG. 4. (a) Temperature T dependence of the total magnetization M_{net}. The solid red line indicates the best fitting based on Eq. (5). (b) Temperature T dependence of the extracted sub-magnetic moments. (c) η with respect to the sample number (the red dot indicates $\eta = 0.19$).

The red line in Fig. 4(a) shows the fitting result based on Eq. (5). By this procedure, we can decouple two submagnetic moments. Figure 4(b) shows the extracted submagnetic moments. The overall trend of each magnetic moment is found to be similar with that in the previous report [27,28]. Then, we obtain $M_{RE}(0) = 0.63$ MA/m, $M_{TM}(0) = 0.55$ MA/m, $\beta_{RE} = 0.43$, and $\beta_{TM} = 0.21$. In the literature, we can also find the Landé g factors of the RE and TM elements, g_{RE} and g_{TM}. Thus, by using these parameters, we can obtain η from the following equation,

$$\eta \equiv \left[1 - (g_{TM}/g_{RE})^{\frac{1}{(\beta_{TM}-\beta_{RE})}}\right][M_{RE}(0)/M_{TM}(0)]^{\frac{1}{(\beta_{TM}-\beta_{RE})}}. \tag{6}$$

Figure 4(c) shows the calculation results of η for each sample and confirms that η is almost invariant irrespective of the samples.

Although we found the linear relation between T_M and T_A in GdFeCo ferrimagnetic materials investigated in the present study, this linearity would not be universal because it needs constant η. However, it should be emphasized that Eq. (3) still enables us to estimate T_A for given materials without a dynamical characterization technique, because T_C, T_M, and η in Eq. (3) can be determined from the temperature dependence of magnetization as shown in Figs. 4(a) and 4(b). Figure 5 shows the relation between the measured angular momentum compensation temperature T_A and the estimated

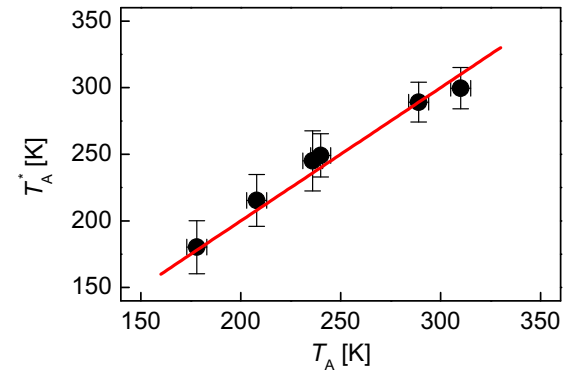

FIG. 5. T_A^* with respect to T_A. The red line is the linear fit with slope = 1 and y-axis interception = 0.

one from Eq. (3), T_A^*. The solid line shows the relation of $T_A^* = T_A$, indicating T_A^* agrees with T_A within experimental errors. It should be noted that Eq. (3) is based on the critical exponent approximation and therefore it cannot be applied to materials with a relatively lower exchange constant between the transition metal and rare earth, such as GdCoNi, in which the critical exponent approximation is not valid [35].

IV. CONCLUSION

In conclusion, we investigate the correlation between T_M and T_A in GdFeCo ferrimagnets. The results show a strong correlation between T_A and T_M, which can be demonstrated experimentally and theoretically. Moreover, a simple yet efficient method was employed for estimating T_A by measuring T_C and T_M. Therefore, this observation will help in easily determining the angular momentum compensation temperature. Accordingly, the proposed scheme can be potentially applied to ferrimagnet-based spintronics devices.

ACKNOWLEDGMENTS

This work was supported by JSPS KAKENHI (Grants No. 15H05702, No. 26870300, No. 26870304, No. 26103002, No. 26103004, No. 25220604, and No. 2604316), Collaborative Research Program of the Institute for Chemical Research, Kyoto University, and R&D project for ICT Key Technology of MEXT from the Japan Society for the Promotion of Science (JSPS). This work was partly supported by The Cooperative Research Project Program of the Research Institute of Electrical Communication, Tohoku University. D.H.K. was supported as an Overseas Researcher under a Postdoctoral Fellowship of JSPS (Grant No. P16314). D.Y.K. and S.B.C. were supported by a National Research Foundations of Korea (NRF) grant funded by the Ministry of Science, ICT, and Future Planning of Korea (MSIP) (2015R1A2A1A05001698 and 2015M3D1A1070465). K.J.K. was supported by the National Research Foundation of Korea (NRF) grant funded by the Korea Government (MSIP) (No. 2017R1C1B2009686, NRF-2016R1A5A1008184) and by the DGIST R&D Program of the Ministry of Science, ICT, and Future Planning (17-BT-02).

D.H.K. conceptualized the work. D.H.K. and T.O. supervised the study. Y.F., H.Y., and A.T. prepared the films and Y.H. and T.O. made the devices. Y.H., D.H.K., D.Y.K., T.O., and T.N. conducted the experiments. D.H.K. and Y.H. performed the analysis, and D.H.K. modeled the data. D.H.K., T.O., S.B.C., and K.J.K. wrote the manuscript. All authors discussed the results and commented on the manuscript.

[1] A. H. MacDonald and M. Tsoi, Philos. Trans. R. Soc. A **369**, 3098 (2011).
[2] S. H. Yang, K.-S. Ryu, and S. Parkin, Nat. Nanotechnol. **10**, 221 (2015).
[3] T. Jungwirth, X. Marti, P. Wadley, and J. Wunderlich, Nat. Nanotechnol. **11**, 231 (2016).
[4] O. Gomonay, T. Jungwirth, and J. Sinova, Phys. Rev. Lett. **117**, 017202 (2016).
[5] T. Shiino, S.-H. Oh, P. M. Haney, S.-W. Lee, G. Go, B.-G. Park, and K.-J. Lee, Phys. Rev. Lett. **117**, 087203 (2016).
[6] S.-H. Oh, S. K. Kim, D.-K. Lee, G. Go, K.-J. Kim, T. Ono, Y. Tserkovnyak, and K.-J. Lee, Phys. Rev. B **96**, 100407(R) (2017).
[7] K.-J. Kim, S. K. Kim, Y. Hirata, S.-H. Oh, T. Tono, D.-H. Kim, T. Okuno, W. S. Ham, S. Kim, G. Go, Y. Tserkovnyak, A. Tsukamoto, T. Moriyama, K.-J. Lee, and T. Ono, Nat. Mater. **16**, 1187 (2017).
[8] I. Radu, K. Vahaplar, C. Stamm, T. Kachel, N. Pontius, H. A. Dürr, T. A. Ostler, J. Barker, R. F. L. Evans, R. W. Chantrell, A. Tsukamoto, A. Itoh, A. Kirilyuk, Th. Rasing, and A. V. Kimel, Nature (London) **472**, 205 (2011).
[9] S. Mangin, M. Gottwald, C.-H. Lambert, D. Steil, V. Uhlíř, L. Pang, M. Hehn, S. Alebrand, M. Cinchetti, G. Malinowski, Y. Fainman, M. Aeschlimann, and E. E. Fullerton, Nat. Mater. **13**, 286 (2014).
[10] C. D. Stanciu, F. Hansteen, A. V. Kimel, A. Kirilyuk, A. Tsukamoto, A. Itoh, and Th. Rasing, Phys. Rev. Lett. **99**, 047601 (2007).
[11] J. Jensen and A. R. Mackintosh, *Rare Earth Magnetism* (Clarendon, Oxford, UK, 1991).
[12] R. K. Wangness, Phys. Rev. **91**, 1085 (1953).
[13] C. D. Stanciu, A. V. Kimel, F. Hansteen, A. Tsukamoto, A. Itoh, A. Kiriliyuk, and Th. Rasing, Phys. Rev. B **73**, 220402(R) (2006).
[14] M. Binder, A. Weber, O. Mosendz, G. Woltersdorf, M. Izquierdo, I. Neudecker, J. R. Dahn, T. D. Hatchard, J.-U. Thiele, C. H. Back, and M. R. Scheinfein, Phys. Rev. B **74**, 134404 (2006).
[15] C. Kaiser, A. F. Panchula, and S. S. P. Parkin, Phys. Rev. Lett. **95**, 047202 (2005).
[16] X. Jiang, L. Gao, J. Z. Sun, and S. S. P. Parkin, Phys. Rev. Lett. **97**, 217202 (2006).
[17] J. Finley and L. Liu, Phys. Rev. Appl. **6**, 054001 (2016).
[18] W. Ham, S. Kim, D.-H. Kim, K.-J. Kim, T. Okuno, H. Yoshikawa, A. Tsukamoto, T. Moriyama, and T. Ono, Appl. Phys. Lett. **110**, 242405 (2017).
[19] K. Ueda, M. Mann, C.-F. Pai, A.-J. Tan, and G. S. Beach, Appl. Phys. Lett. **109**, 232403 (2016).
[20] K. Ueda, M. Mann, P. W. P. de Brouwer, D. Bono, and G. S. D. Beach, Phys. Rev. B **96**, 064410 (2017).
[21] N. Roschewsky, T. Matsumura, S. Cheema, F. Hellman, T. Kato, S. Iwata, and S. Salahuddin, Appl. Phys. Lett. **109**, 112403 (2016).
[22] R. Mishra, J. Yu, X. Qiu, M. Motapothula, T. Venkatesan, and H. Yang, Phys. Rev. Lett. **118**, 167201 (2017).
[23] T. Okuno, K.-J. Kim, T. Tono, S. Kim, T. Moriyama, H. Yoshikawa, A. Tsukamoto, and T. Ono, Appl. Phys. Express **9**, 073001 (2016).
[24] K.-J. Kim, J.-C. Lee, S.-B. Choe, and K.-H. Shin, Appl. Phys. Lett. **92**, 192509 (2008).
[25] D.-H. Kim, K.-W. Moon, S.-C. Yoo, B.-C. Min, K.-H. Shin, and S.-B. Choe, IEEE Trans. Magn. **49**, 3207 (2013).
[26] J.-C. Lee, K.-J. Kim, J. Ryu, K.-W. Moon, S.-J. Yun, G.-H. Gim, K.-S. Lee, K.-H. Shin, H.-W. Lee, and S.-B. Choe, Phys. Rev. Lett. **107**, 067201 (2011).
[27] T. A. Ostler, R. F. L. Evans, R. W. Chantrell, U. Atxitia, O. Chubykalo-Fesenko, I. Radu, R. Abrudan, F. Radu, A.

Tsukamoto, A. Itoh, A. Kirilyuk, T. Rasing, and A. Kimel, Phys. Rev. B **84**, 024407 (2011).
[28] A. Kirilyuk, A. V. Kimel, and Th. Rasing, Rep. Prog. Phys. **76**, 026501 (2013).
[29] S. Chikazumi, in *Physics of Ferromagnetism* (Clarendon Press, Oxford, UK, 1997), p. 128.
[30] C. Kittel, Phys. Rev. **76**, 743 (1949).
[31] G. G. Scott, Rev. Mod. Phys. **34**, 102 (1962).
[32] B. I. Min and Y.-R. Jang, J. Phys.: Condens. Matter **3**, 5131 (1991).
[33] D. Chiba, S. Fukami, K. Shimamura, N. Ishiwata, K. Kobayashi and T. Ono, Nat. Mater. **10**, 853 (2011).
[34] R. Hasegawa, R. J. Gambino, and R. Ruf, Appl. Phys. Lett. **27**, 512 (1975).
[35] R. Hasegawa and R. C. Taylor, J. Appl. Phys. **46**, 3606 (1975).

Correction: Some entries in the second column of Table I contained errors and have been corrected.

Correction: The email address of the second author was no longer valid and has now been updated.